THE SECONDARY DISCHARGE SUPPORTED BY MICRODISCHARGE IN VORTEX FLOW

Ok.V. Solomenko, V.V. Lendiel, V.Ya. Chernyak, D.O. Kalustova, V.V. Iukhymenko, E.V. Martysh, I.V. Prysiazhnevych, V.O. Shapoval

Taras Shevchenko National University of Kyiv, Ukraine

E-mail: chernyak_v@ukr.net; oksana_solomenko@ukr.net

This research studies the DC microdischarges properties in the air vortex flow. The electrical parameters of the discharge and optical characteristics of the microdischarge plasma jet have been studied. The electronic excitation temperatures has been determined by Boltzmann plots using oxygen atom multiplets (777, 844, 926 nm). Also, there are the molecular bands of NO, OH, and N_2 (B-A) and N_2 (C-B) in the microdischarge plasma spectrum. The vibrational and rotational excitation temperatures have been determined.

PACS: 52.50.Dg; 52.80.-s

INTRODUCTION

Plasma generators of non-equilibrium atmospheric pressure plasma attract the most attention from a wide group of experts from various areas. This is due to the possibility of technological applications of such plasma sources and disclosure of fundamental questions regarding the mechanisms of plasma interaction with living organisms (Plasma medicine).

Atmospheric pressure plasma has a wide range of applications in industries ranging from electronics to medicine. Promising task is to obtain nanomaterials without bulky expensive equipment. This problem can be solved by using non-equilibrium atmospheric pressure plasma, which can be obtained by using various categories such as barrier discharge [1], corona discharge [2], etc. But among the existing types of discharges greatest interest is microdischarges because it is a non-equilibrium plasma generator, similar to the plasma glow discharge low pressure [3]. It has a small size and does not require a high power. Also, unlike corona discharge, in this discharge gas stream may be directly involved in the discharge (through a tubular electrode) that promotes the synthesis and processing of nanomaterials [4, 5]. In addition, various gas mixtures can be used to generate the microplasma jets.

Virtually unexplored the secondary discharges which supported by plasma of microdischarges. It is known [6] that the secondary discharge provides the ability to create potential leaping near the electrode of the secondary discharge. This can lead to the empowerment of an applications number of microdischarge plasma.

This work is devoted to the researching of electrical properties of DC microdischarge in the vortex air flow that generated plasma jet with radius ~ 1 mm in atmospheric pressure area. In this work examine two cases: 1–there are no electric field in outlet area; 2–there is specially created constant electric field. The last case corresponds to the secondary microdischarge, which is supported by the microdischarge plasma jet.

1. EXPERIMENTAL SETUP

The scheme of the experimental setup that was used in researches of microdischarge jet is shown in Fig. 1.

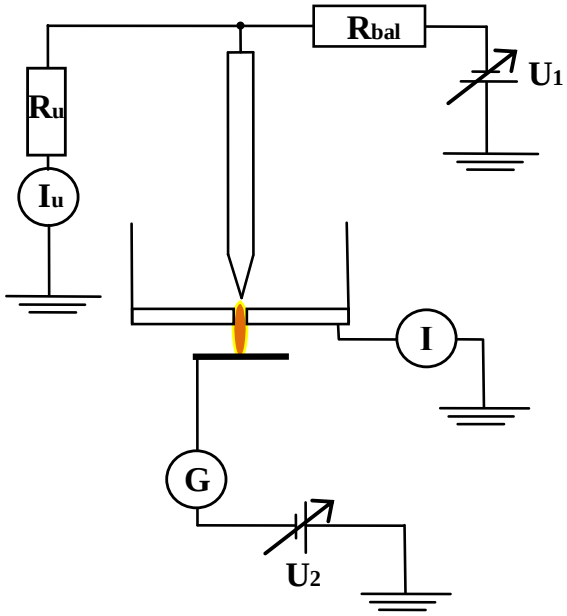

Fig. 1. The electrical scheme of generating of the microdischarge jet

The generator of the microdischarge jet was the axially symmetric system. The copper electrodes (the high voltage electrode with a diameter of 6 mm and an output electrode with a thickness of 1 mm) were located at a distance of 1 mm. The high voltage electrode has cylindrical form with cone-shaped ending. The height of cone-shaped ending was 8 mm and the radius of curvature ~0.5 mm. Both electrodes were water-cooled. Air was used as working gas and it was injected tangential to the device lateral surface.

2. RESULTS AND DISCUSSION

In this study, the current-voltage characteristics (CVC) measurements of self-microdischarge were performed for different air flows (G = 1…3 l / min) and for different output diameters (from which microdischarge jet was blown out): d = 0.5 mm or d = 1.7 mm. The output (external) electrode of the design was grounded.

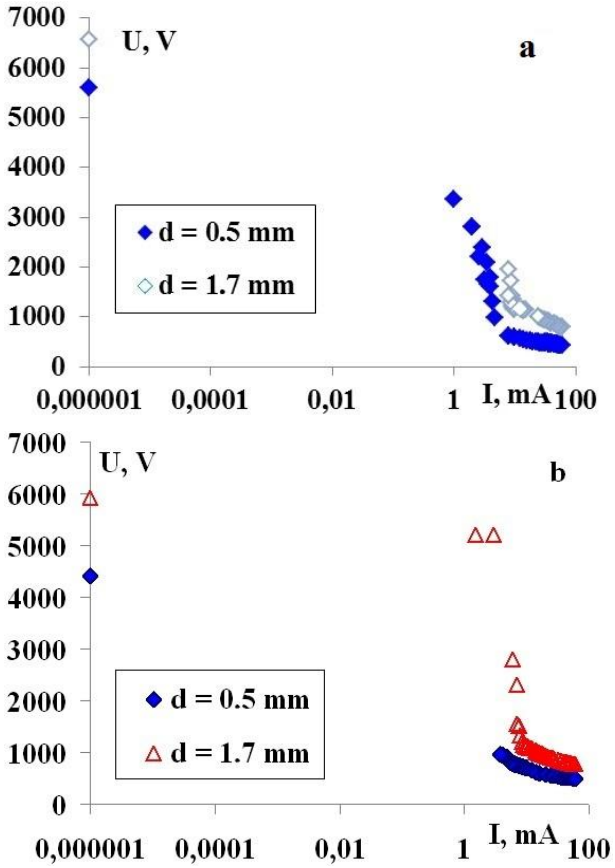

Fig. 2. CVC of the microdischarge that measured for the constructions d = 0.5 mm and d = 1.7 mm

It should be noted that increasing of outlet diameter (d) in output electrode leads to contraction of microplasma jet. Its form is similar to the rotating gliding discharge. The measuring results of CVC are demonstrated in Fig. 2. The measuring results of CVC with the positive potential of the high voltage electrode are presented in Fig. 2,a. The gas flows are the same under different outlet diameters and correspond to G = 1 l / min. In Fig. 2,b the negative potential of the high voltage electrode and the gas flows in the system was varied: in case of d = 0.5 mm air flow corresponds to G = 1 l/min; for d = 1.7 mm – G = 3 l/min. The extreme points on the ordinates axis correspond to the breakdown voltage.

As it can be seen from Fig. 2, the CVC has monotone character and does not depend on the plasma jet outlet diameter d. The form of the CVC reminds transition from Townsend dark discharge (at low currents) to normal glowing discharge (started from ~ 10 mA or more). This transition is crossing through subnormal glowing discharge. It was found that compared with d = 0.5 mm increasing of d leads to higher voltages of the microdischarge burning.

The secondary microdischarge (SMD) generation was supported by the microplasma flow. The nickel plate (diameter of 10 mm and a thickness of 0.1 mm) served as an electrode of the secondary discharge during the SMD generation. Measurements were performed for different distances between the electrode of the secondary discharge and the surface of the output electrode of the self-microdischarge.

The parameters of the self-microdischarge circuit are remained unchanged. Measurements were carried out in the air flow G = 1 l / min. The results of the measurement for CVC of SMD for d = 0.5 mm with the positive potential of the high voltage electrode are presented in Fig. 3. The CVC of the SMD has a view similar to the probe characteristics.

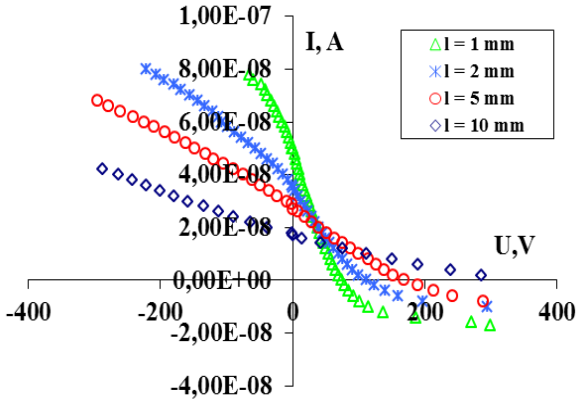

Fig. 3. CVC of the secondary microdischarge (SMD) for different distances between the secondary electrode and the surface of the output electrode at the d = 0.5 mm; the self-microdischarge had I = 20 mA

The measurements of the SMD plasma jet emission were performed perpendicular to its axis on the distance 1…2 mm from the output electrode surface. Distance between the plasma jet and inlet of the quartz optical fiber was about 12…13 mm. Also measurements were carried out at distance of 2.5 mm between the secondary electrode and the surface of the output electrode.

One can in Fig. 3 a saturation regions can be observed on the current-voltage characteristics of the secondary discharge for any potential of the electrode of the secondary discharge. The magnitude of the saturation current significantly depends on the polarity of the voltage on the electrode of the secondary discharge. In case of positive potential of the high voltage electrode the saturation current of the secondary discharge with the negative polarity is much higher than in the positive polarity. In case of negative potential of the high voltage electrode the saturation current of the secondary discharge is much higher at the positive polarity. The direction of the secondary discharge current at the higher saturation of the current coincides with the direction of the self-microdischarge current.

It was found that emission spectra of the plasma jet and emission spectra of the SMD at E = 0 (no secondary Ni electrode) and E ≠ 0 (SMD) are almost identical. The measurements of the microplasma emission spectrum was carried out at discharge currents I = 30 mA (Fig. 4,a) and I = 8.5 mA (Fig. 4,b). These two regimes correspond to normal glowing discharge and subnormal glowing discharge respectively.

Optical emission spectroscopy of generated plasma jet was made by CCD-based spectrometer Solar TII in the wavelength range of 200…1100 nm with spectral resolution ~ 0.2 nm. Emission spectra of the microplasma showed the presence of atomic oxygen multiplets (777, 844 and 926 nm) and molecular bands of NO, OH, N_2 (B-A) and N_2 (C-B) and also N_2^+.

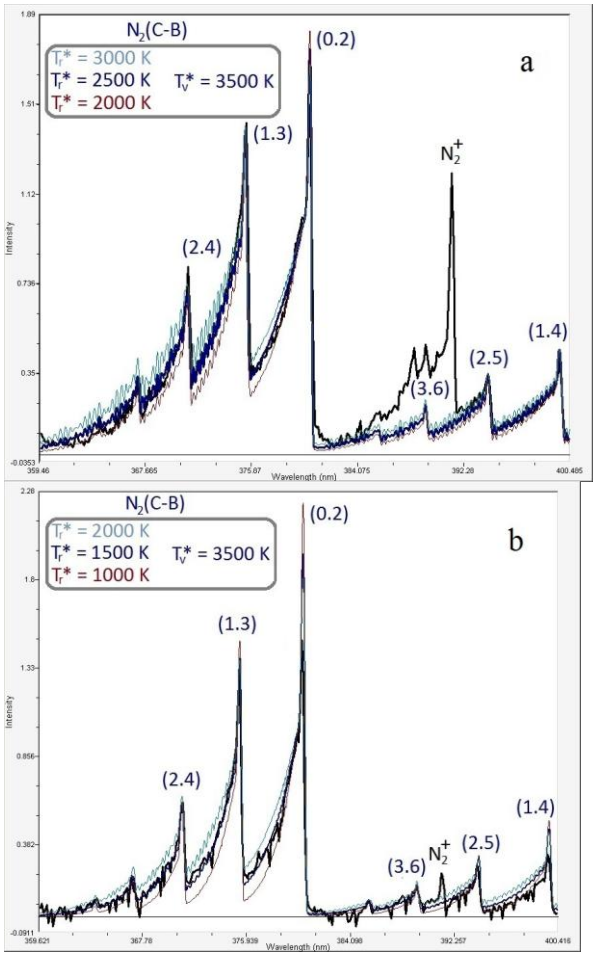

Fig. 4. Comparison of the experimental emission spectra (black) with simulation spectra of N_2 (C-B) created in Specair code. Discharge current I = 30 мА (a) and I= 8.5 мА (b)

The temperature of excited vibrational (T_v^*) and rotational (T_r^*) levels of N_2 and OH molecules were determinated by comparing the experimental spectra with spectra simulation in Specair code. In case of I = 30 mA, when d = 1.7 mm, the temperatures of N_2 and OH molecules: $T_r^*(N_2) = T_r^*(OH) = 2500 \pm 500$ K: $T_v^*(N_2) = T_v^*(OH) = 3500 \pm 500$ K (see Fig. 4,a). In case of a discharge current of 8.5 mA (for the same outlet diameter) the temperatures of N_2 and OH were (Fig. 4,b):$T_r^*(N_2) = 1500 \pm 500$ K,$T_v^*(N_2) = 3500 \pm 500$ K and $T_r^*(OH) = 2000 \pm 500$ K, $T_v^*(OH) = 3500 \pm 500$ K.

Temperature of excited electronic population levels (T_e^*) was determined for the case of I = 30 mA, when d = 1.7 mm. The oxygen $T_e^*(O)$ has been defined by the Boltzmann plots method. The three most intense multiplets (777.2, 844, 926 nm) are used in this method. Also T_e^* was determined from the first (N_2 (B-A)) and second (N_2 (C-B)) positive systems of nitrogen radiation intensities ratio. Temperatures among themselves varied greatly, namely: $T_e^*(O) = 4500$ K, $T_e^*(N_2) = 9000 \pm 1000$ K.

Also in case of I = 30 mA, when d = 1.7 mm using determined temperatures it was created the simulated spectrum of the microplasma. It is represented in Fig. 5.

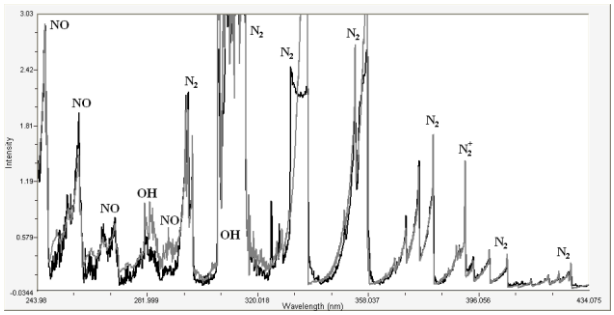

Fig. 5 Comparison of experimental (black) spectrum of microplasma and simulated (gray) spectrum at temperatures: $T_r^*(N_2) = 2500$ K, $T_v^*(N_2) = 3500$ K and $T_e^*(N_2) = 9000$ K

CONCLUSIONS

Thus, it was found that:

• in case of the microplasma jet, which is blown out from the hole, its diameter affects significantly on the plasma jet shape;

• the transition through the zero at current-voltage characteristic of the secondary discharge depends on the distance between the surface of the output electrode and the electrode of the secondary discharge;

• a saturation regions can be observed on the current-voltage characteristics of the secondary discharge for any potential of the electrode of the secondary discharge. The magnitude of the saturation current significantly depends on the polarity of the voltage on the electrode of the secondary discharge. In case of positive potential of the high voltage electrode the saturation current of the secondary discharge with the negative polarity is much higher than in the positive polarity. In case of negative potential of the high voltage electrode the saturation current of the secondary discharge is much higher at the positive polarity. The direction of the secondary discharge current at the higher saturation of the current coincides with the direction of the self-microdischarge current;

• emission spectra of the plasma jet and emission spectra of the secondary microdischarge at E = 0 (no secondary electrode) and E ≠ 0 (the secondary microdischarge) are almost identical;

• the temperatures T_v^* and T_r^* were determined from N_2 (C-B) and OH (A-X) bands at hole diameter d = 1.7 mm. They are similar in values.

REFERENCES

1. D. Lanbo, Z. Xiuling, X. Zhijian. Preparation of copper nanoparticles using dielectric barrier discharge at atmospheric pressure and its mechanism// *Plasma Science and Technology*. 2014, № 1, p. 41-44.
2. S.N. Abolmasov, L. Kroely, et al. Negative corona discharge: application to nanoparticle detection in rf reactors// *Plasma Sources Sci. Technol.* 2009, p. 6.
3. K.H. Becker, U. Kogelschatz, et al. Non-equilibrium air plasma at atmospheric pressure // *Institute of Physics Publishing, Bristol and Philadelphia*. 2005.
4. R.M. Sankaran, D. Holunga, et al. Synthesis of blue luminescent Si nanoparticles using atmospheric-pressure microdischarges // *NANO LETTERS (5)*. 2005, № 3, p. 537-541.
5. W.-H. Chiang, R.M. Sankaran. Microplasma synthesis of metal nanoparticles for gas-phase studies of catalyzed carbon nanotube growth // *Applied Physics Letters (91)*. 2007.
6. V. Prysiazhnevych, V.Ya. Chernyak, et al. Optical and probe diagnostics of plasma-liquid systems with secondary discharge // *Problems of Atomic Science and Technology*. 2007, p. 212-215.

Article received 21.09.2014

ВТОРИЧНЫЙ РАЗРЯД, ПОДДЕРЖИВАЕМЫЙ МИКРОРАЗРЯДОМ В ВИХРЕВОМ ПОТОКЕ

Ок.В. Соломенко, В.В. Лендьел, В.Я. Черняк, Д.О. Калустова, В.В. Юхименко, Е.В. Мартыш, И.В. Присяжневич, В.О. Шаповал

Исследованы свойства микроразрядов постоянного тока в вихревом потоке воздуха, а также электрические параметры этого разряда и оптические характеристики плазменного факела микроразряда. Температуру заселения возбужденных электронных уровней определяли с помощью диаграмм Больцмана, используя мультиплеты атома кислорода (777, 844, 926 нм). В спектре плазмы микроразряда присутствуют молекулярные полосы NO, OH, N_2 (B-A) и N_2 (C-B). Определены температуры заселения колебательных и вращательных уровней.

ВТОРИННИЙ РОЗРЯД, ЩО ПІДТРИМУЄТЬСЯ МІКРОРОЗРЯДОМ У ВИХРОВОМУ ПОТОЦІ

Ок.В. Соломенко, В.В. Лен д'єл, В.Я. Черняк, Д.О. Калустова, В.В. Юхименко, Є.В. Мартиш, І.В. Присяжневич, В.О. Шаповал

Дослідженню властивості мікророзрядів постійного струму у вихровому потоці повітря, а також електричні параметри цього розряду та оптичні характеристики плазмового факелу мікророзряду. Температура заселення збуджених електронних рівнів визначалася за допомогою діаграм Больцмана, з використанням мультиплетів атома кисню (777, 844, 926 нм). У спектрі плазми мікророзряду присутні молекулярні смуги NO, OH, N_2 (B-A) і N_2 (C-B). Визначені температури заселення коливальних та обертальних рівнів.